Supporting information

Highly durable and sustainable copper-iron-tin-sulphide (Cu_2FeSnS_4) anode for Li-ion battery: Effect of operating temperatures

Akbar I. Inamdar,[1,*] Amol S. Salunke[1], Bo Hou,[2,§], Nabeen K. Shrestha,[1] Hyunsik Im[1,*] Hyungsang Kim[1,*]

[1]Division of Physics and Semiconductor Science, Dongguk University, Seoul 04620, Republic of Korea

[2] Department of Engineering Science, University of Oxford, Parks Road, OX1 3PJ, UK

[§] Present address: School of Physics and Astronomy, Cardiff University, Cardiff, CF24 3AA, Wales, UK.

Keywords: Li-ion Batteries, quaternary Cu_2FeSnS_4 anode, long cycle life, temperature effect

***Corresponding Authors**

[*]E-mail: akbarphysics2002@gmail.com, hyunsik7@dongguk.edu, hskim@dongguk.edu

(a)

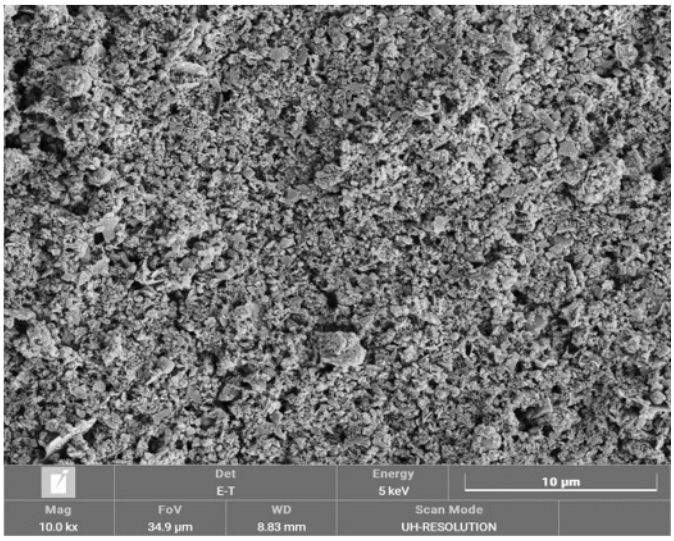

(b)

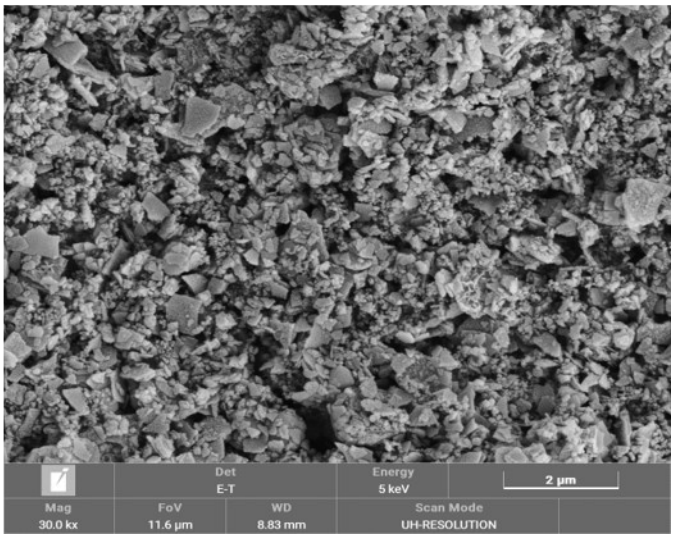

Figure S1. Scanning electron microscopy (SEM) images (at different magnifications) of the CFTS powder coated onto the Cu foil paper. Grains of different sizes and randomly shaped plates are distributed all over the sample.

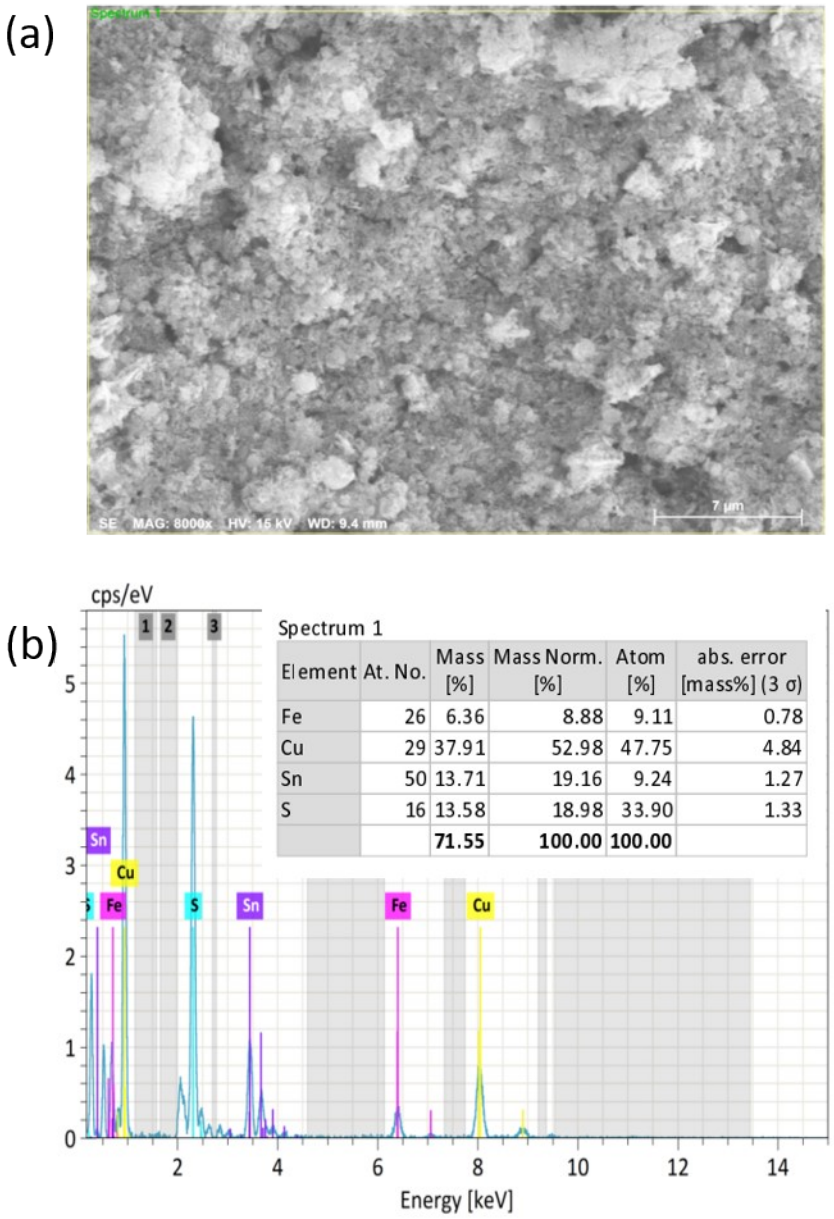

Figure S2. Energy dispersive X-ray analysis (EDAX) of the CFTS anode. (a) SEM image of the point at which the EDAX measurements are performed. (b) EDAX spectra revealing the presence of Cu, Fe, Sn, and S in the sample. The inset presents the relative compositions of the elements.

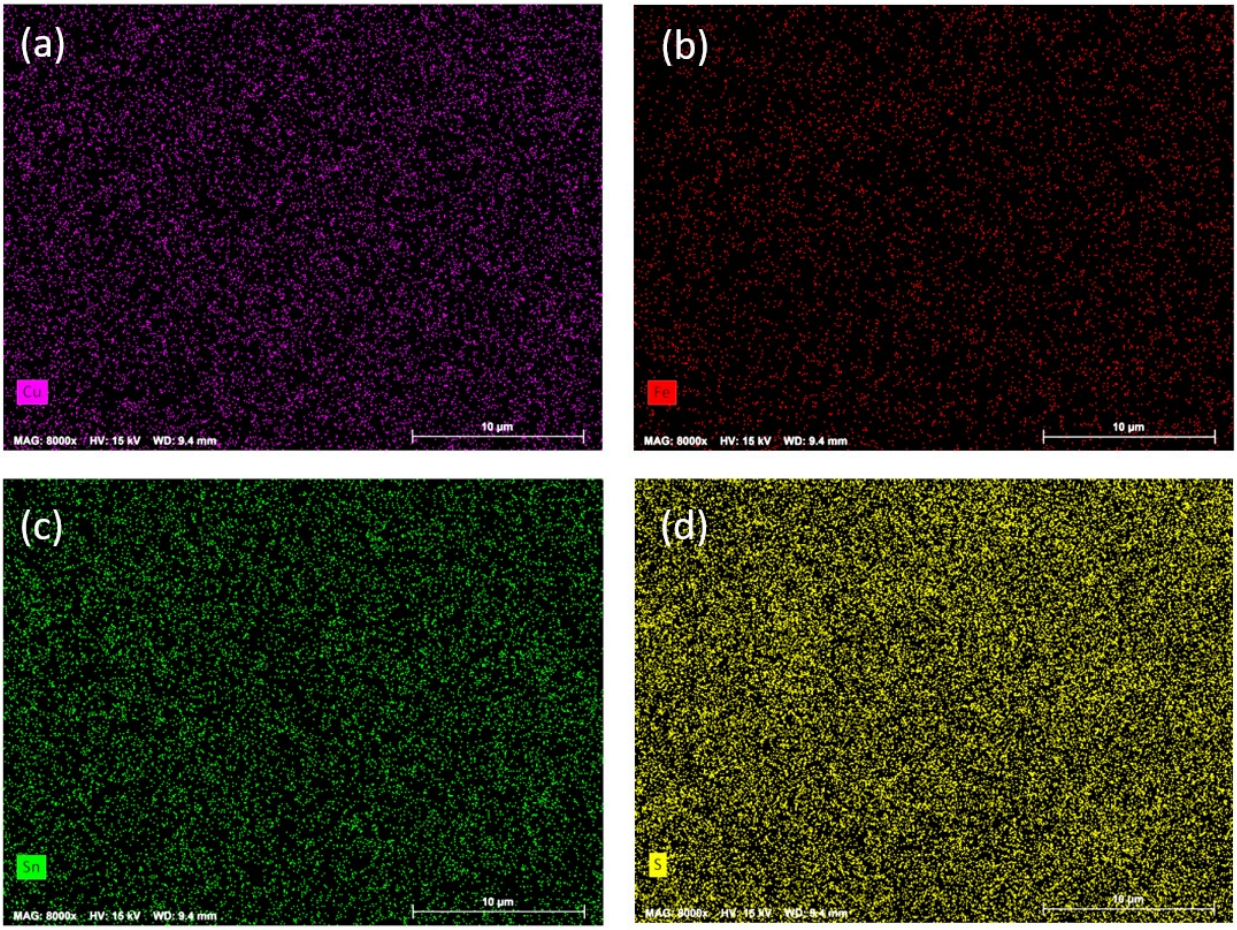

Figure S3. EDAX elemental mapping of the CFTS anode, suggesting the uniform distribution of Cu, Fe, Sn, and S in the sample.

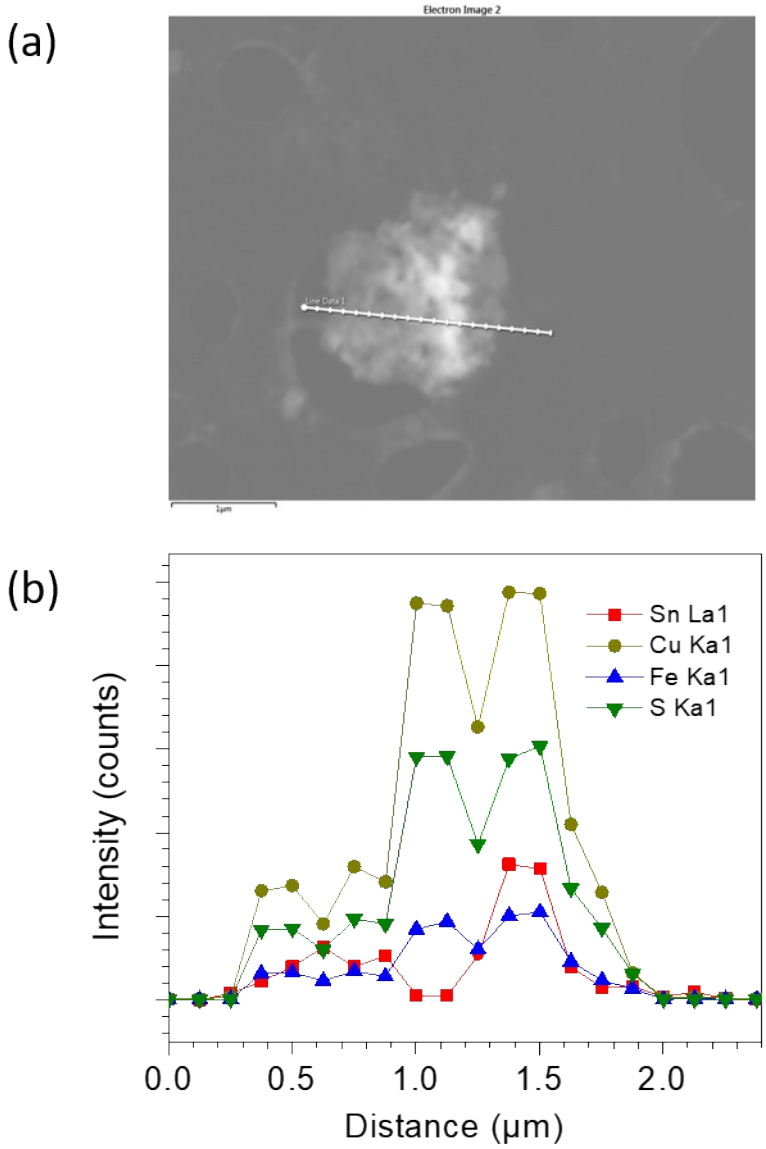

Figure S4. (a) High-angle annular dark-field-scanning transmission electron microscopy (HAADF-STEM) image in the region where the STEM elemental line scan profile was recorded (b) Line-scanning profiles of Cu, Fe, Sn, and S.

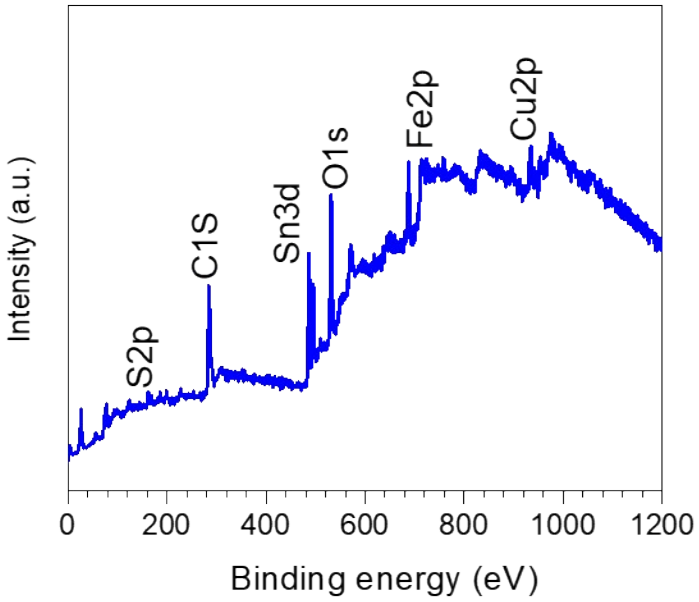

Figure S5. X-ray photoelectron spectroscopy (XPS) survey spectrum of the CFTS anode, revealing the presence of the desired elements.

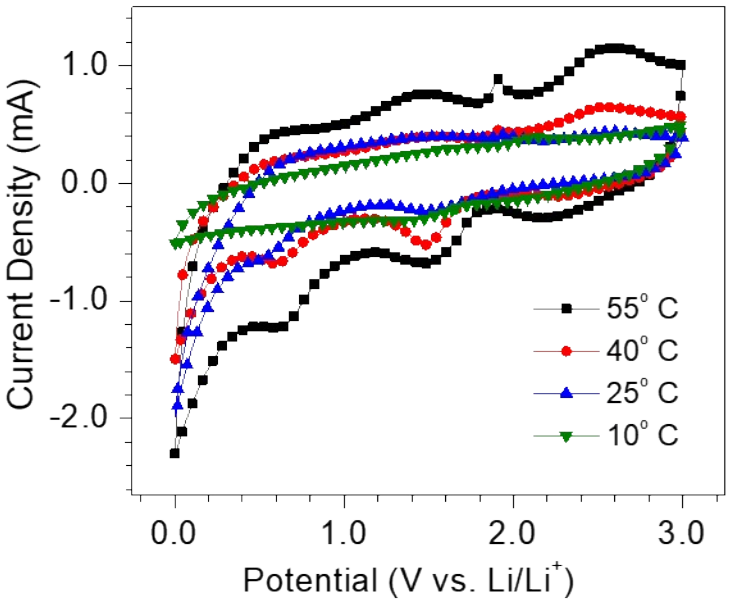

Figure S6. CV curve of the CFTS anode recorded at different temperatures in the potential window between 0.01 and 3.0 V (vs. Li/Li^+) at a scan rate of 0.1 mVs^{-1}.

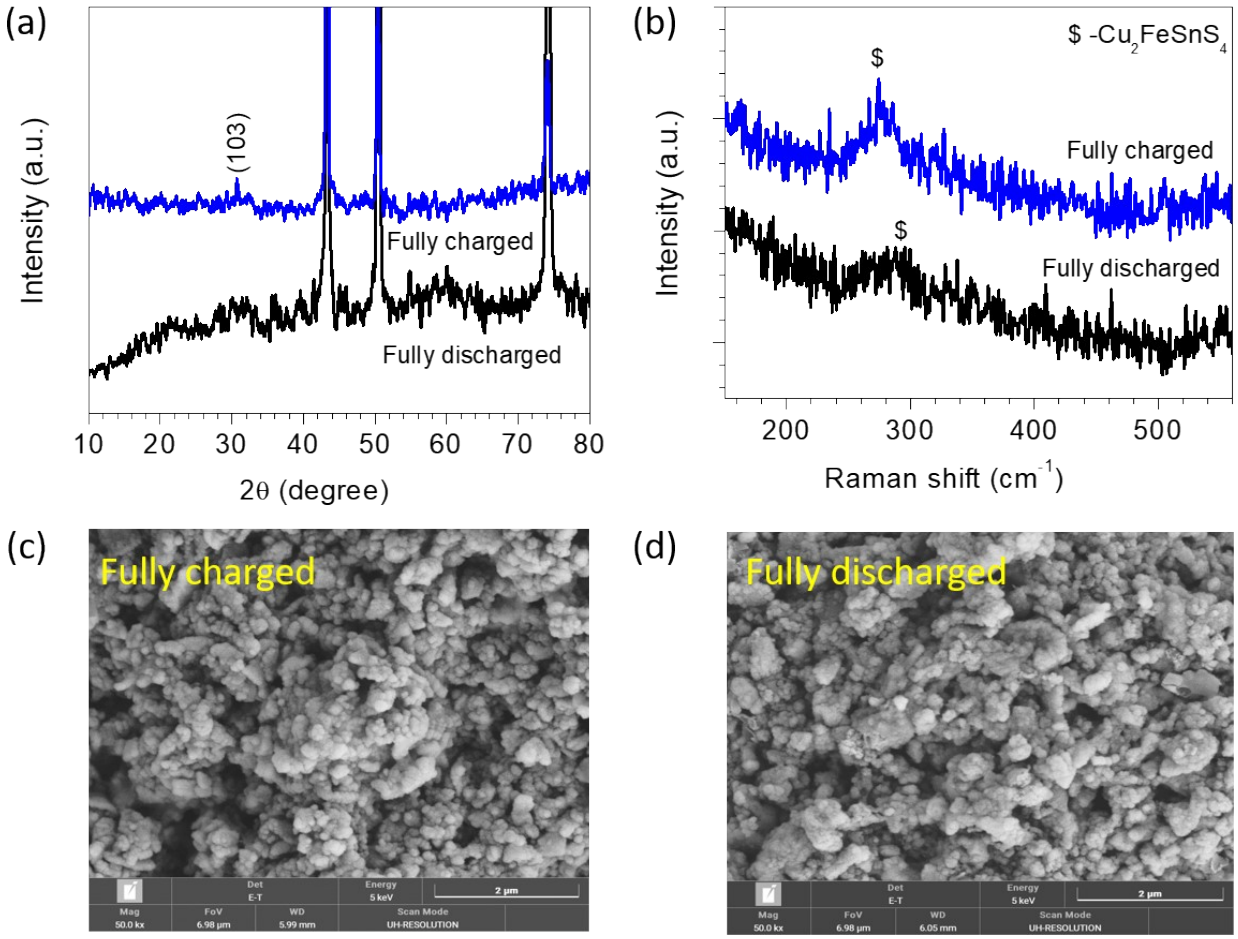

Figure S7. Ex situ (a) X-ray diffraction spectra, (b) Raman spectra, and (c, d) SEM morphologies of the CFTS anode in the fully charged to 3.0 V and fully discharged to 0.01 V states.

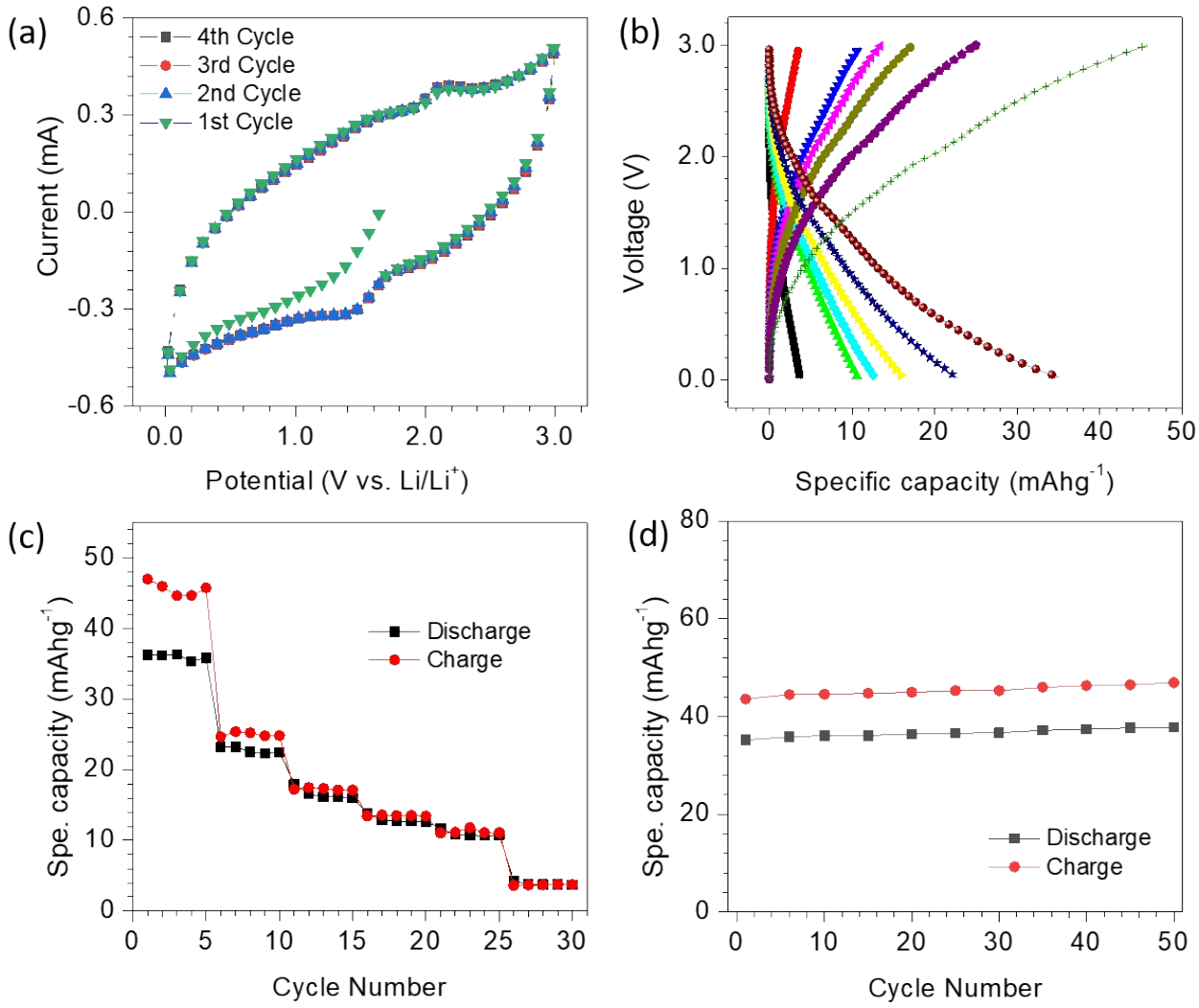

Figure S8. Electrochemical characteristics of the CFTS anode at an operating temperature of 10 °C: (a) Five CV curves recorded at a scan rate of 0.1 mVs^{-1}, (b) Galvanostatic charge–discharge (GCD) characteristics at a current of 0.1 Ag^{-1}, (c) rate performances at different currents, and (d) long-life-cycling performance.

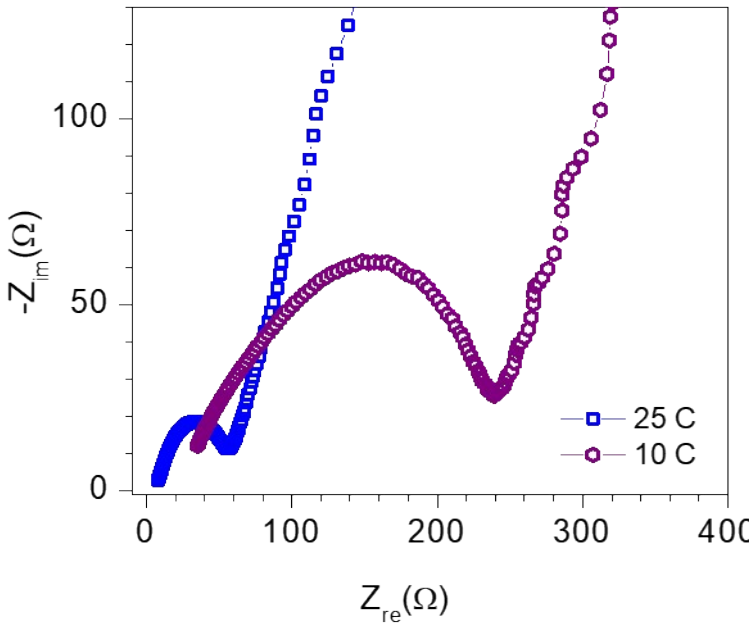

Figure S9. Nyquist plots of the CFTS anode recorded at 10 °C and 25 °C, revealing the effect of the temperature on the charge transfer resistance.

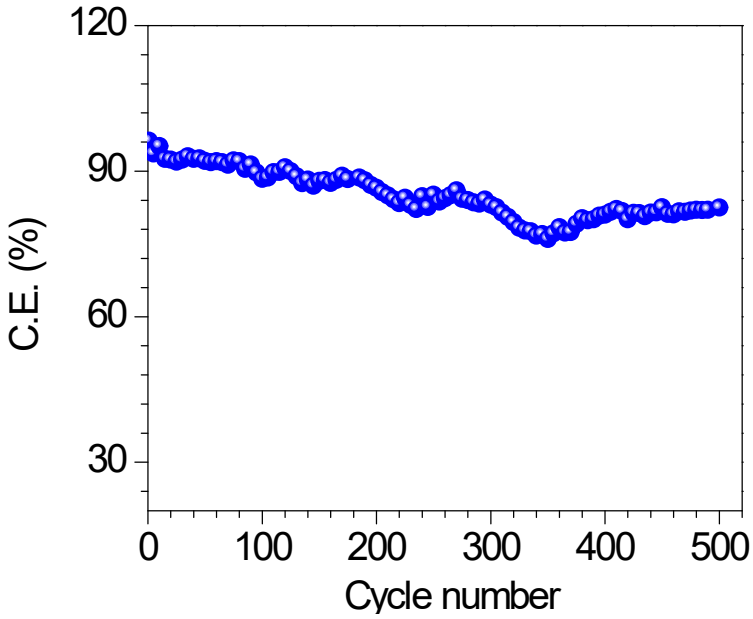

Figure S10. Coulombic efficiency of the CFTS anode electrode studied at 25 °C, for 500 charge discharge cycles.

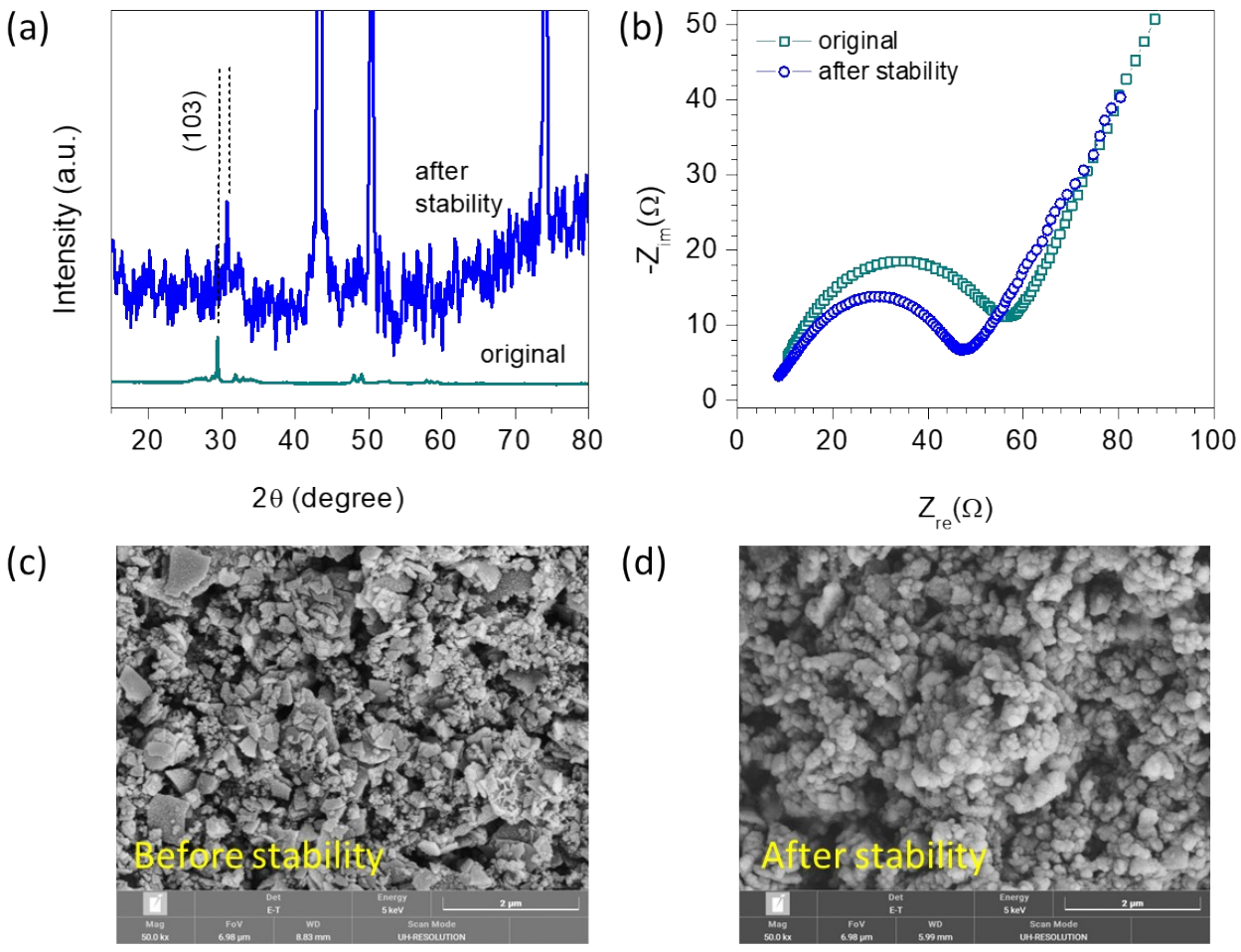

Figure S11. (**a**) XRD patterns of the CFTS anode electrode recorded before after prolonged stability measurements of 500 cycles, (**b**) Nyquist plot before and after stability of 500 cycles, (**c,d**) SEM images of the CFTS before and after stability test.

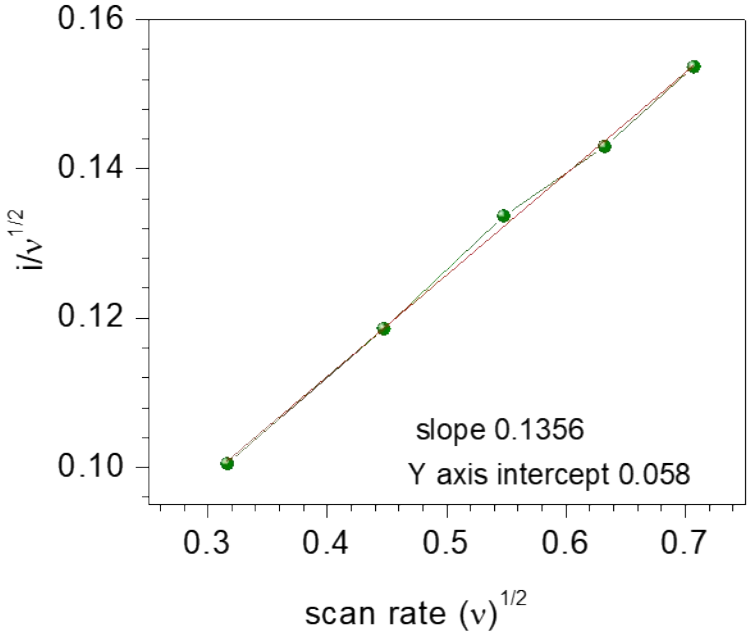

Figure S12. Plot of $v^{1/2}$ vs. $i/v^{1/2}$, from which the fitting parameters k_1 and k_2 are estimated as the slope of the curve and y-axis intercept, respectively.